Dynamic Article Links ▶

PAPER

Silver(I) complexes of 9-anthracenecarboxylic acid and imidazoles: synthesis, structure and antimicrobial activity†

Malachy McCann,[a] Robert Curran,[a] Marcia Ben-Shoshan,[a] Vickie McKee,*[b] Asif Ali Tahir,[b] Michael Devereux,[c] Kevin Kavanagh,[d] Bernadette S. Creaven[e] and Andrew Kellett[f]

[Ag₂(9-aca)₂] (**1**) (9-acaH = 9-anthracenecarboxylic acid) reacts with a series of imidazoles to give [Ag(imidH)$_{2.3}$(CH₃CN)$_{0.7}$](9-aca) (**3**), [Ag₆(imidH)₄(9-aca)₆(MeOH)₂] (**4**), {[Ag(1-Me-imid)₂]₂[Ag₄(9-aca)₆]} (**5**), {[Ag(1-Bu-imid)₂]₂[Ag₄(9-aca)₆]} (**6**) and [Ag(apim)](9-aca)·H₂O (**7**) (imidH = imidazole; 1-Me-imid = 1-methylimidazole; 1-Bu-imid = 1-butylimidazole; apim = 1-(3-aminopropyl)imidazole). The mononuclear complex **3**, hexanuclear **4–6**, and polymeric **7**, were all characterised using X-ray crystallography. While many of the complexes possess excellent *in vitro* antifungal and antibacterial activities they are, unanimously, more effective against fungal cells. The insect, *Galleria mellonella*, can survive high doses of the Ag(I) complexes administered *in vivo*, and a number of the complexes offer significant protection to larvae infected with a lethal dose of pathogenic *Candida albicans* cells.

Introduction

Pathogenic fungi and bacteria cause many infectious diseases in both immunosuppressed and immunocompetent individuals. Additionally, infections with resistant microorganisms are often associated with high rates of morbidity and mortality and also increase health care treatment costs.[1–4] In recent times, there has been something of a renaissance in the use of nanoparticulate silver(0) and silver(I) complexes to prevent and to treat stubborn microbial infections. Despite the fact that microbial resistance to Ag(I) is relatively rare, Ag(I)-resistance genes have been identified, giving rise to concerns over the widespread use of clinical and hygiene products containing silver.[5] Although a small number of people experience delayed sensitivity to silver, the metal and its monocation do not present a serious toxic risk to any organ system in the human body.[6]

The Ag(I) ion is now the active agent in many healthcare products such as silver-coated catheters,[7] wound dressings[8,9] and burn treatment creams.[10] Evidence has been provided[11] for the antifungal activity of a burn wound dressing coated with AgNO₃ against *Candida albicans*, *C. glabrata*, *C. tropicalis* and *Saccharomyces cerevisiae*. Ag(0) nanoparticles have been incorporated into a topical antimicrobial gel and demonstrated potent activity against *Aspergillus niger* and *C. albicans*.[12] The antimicrobial effects of medical devices containing Ag(0) have formed the basis of a recent review which highlights the growing importance of materials that prevent microbial surface adhesion.[13]

The Ag(I) ion is known to interfere with electron transport[14] and alter the respiration of *C. albicans* cells.[15] McCann and co-workers suggested that the interaction of Ag(I) and the mitochondrion,[14–16] coupled with the generation of lipid peroxides,[14] was evidence for the generation of free radicals. More recently,[17] it has been demonstrated that *C. albicans* cells respond to AgClO₄ by activating an oxidative stress response *via* phosphorylation of a high osmolarity protein (Hog1P) and nuclear translocation of the *C. albicans* activating protein-1 (Cap1p). The high antimicrobial efficacy of tetrahedral, Ag(I) bis-phosphine[18] and *N*-heterocyclic carbene[19] complexes has been demonstrated. Li and coworkers[20] reported that the hexanuclear Ag(I) complex, [Ag₆L₆]·4DMF (HL = 2-thiophene *N*(4)-methylthiosemicarbazone), showed moderate activity against Gram negative and Gram positive bacteria with MIC₁₀₀ values (minimum inhibitory concentration of complex required for 100% retardation of bacterial cell growth) ≥0.5 μg cm⁻³ and displayed poor growth inhibition towards the fungi, *C. albicans* and *C. lusitaniae*. In recent studies, [Ag₂(phen)₃(mal)]·2H₂O (phen

ᵃDepartment of Chemistry, National University of Ireland, Maynooth, Co. Kildare, Ireland
ᵇChemistry Department, Loughborough University, Loughborough, Leics., LE11 3TU, UK. E-mail: v.mckee@lboro.ac.uk
ᶜThe Inorganic Pharmaceutical and Biomimetic Research Laboratory, Focas Institute, Dublin Institute of Technology, Kevin St., Dublin 2, Ireland
ᵈDepartment of Biology, National University of Ireland, Maynooth, Co. Kildare, Ireland
ᵉCentre of Applied Science for Health, Institute of Technology Tallaght, Dublin, Dublin 24, Ireland
ᶠSchool of Chemical Sciences and National Institute for Cellular Biotechnology, Dublin City University, Glasnevin, Dublin 9, Ireland

= 1,10-phenanthroline; malH$_2$ = malonic acid) was shown to inhibit the growth of *C. albicans*, by affecting mitochondrial function, retarding cytochrome synthesis, uncoupling cellular respiration and causing gross distortions in cell morphology.[21] The mononuclear complex, [Ag(phendio)$_2$]ClO$_4$ (phendio = 1,10-phenanthroline-5,6-dione), strongly inhibited the growth of *C. albicans* and caused extensive, non-specific DNA cleavage in the organism.[22] Against the same fungi, the Ag(I) salicylate complexes, [Ag$_2$(salH)$_2$] and [Ag$_2$(NH$_3$)$_2$(salH)$_2$] (salH$_2$ = salicylic acid), had MIC$_{100}$ values of 5.0 and 0.5 μM, respectively.[23]

Investigations into the effects of silver(I) ions on bacterial cells revealed that they interact with the respiratory chain of *Escherichia coli*[24] and can lower the content of phospholipid fatty acids in some metal-reducing bacteria.[25] Electron microscopy and X-ray microanalysis have shown that silver builds up as granules in the cell wall and in the cytoplasm of *E. coli* and *Staphylococcus aureus*,[26,27] inflicting damage to the RNA and DNA and also deactivating cellular proteins. The most widely known bactericidal mechanism of the Ag(I) ion is its interaction with the thiol group of the L-cysteine residue of proteins and consequent enzyme inactivation.[28–30] Other Ag(I) bactericidal mechanisms, such as K$^+$ ion release,[31] bonding to DNA[32] and the generation of intracellular reactive oxygen species,[24,33,34] have also been reported.
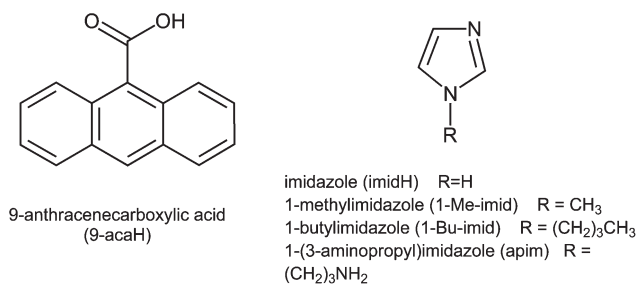

Fig. 1 Ligand structures.

In 2007, we reported[35] the structures and biological activities of dinuclear and tetranuclear Ag(I) complexes containing the 9-anthracenecarboxylate anion (9-acaH = 9-anthracenecarboxylic acid (Fig. 1)). [Ag$_2$(9-aca)$_2$] (**1**) was found to be very active against the bacterial species *E. coli* and methicillin-resistant *S. aureus* (MRSA) (MIC$_{50}$ = 22.44 and 11.36 μM, respectively) and against the fungus *C. albicans* (MIC$_{100}$ = 0.95 μM). However, the tetranuclear, amine complex, [Ag$_4$(9-aca)$_4$(NH$_3$)$_2$] (**2**), displayed enhanced activity universally against the microbial cells (corresponding inhibitory concentrations were 8.51, 5.44 and 0.14 μM, respectively).[35] The significant improvement in biological activity witnessed upon the introduction of the NH$_3$ ligands in **2** and in [Ag$_2$(NH$_3$)$_2$(salH)$_2$][23] was the stimulus for the present work.

Herein, we report the synthesis, structures and *in vitro* antimicrobial effects of a series of new Ag(I) complexes containing both the 9-aca$^-$ anion and N-donor ligands based on imidazole (Fig. 1). Metal complexes containing imidazole-based ligands are also of interest because the imidazole ring is an essential metal binding site in many metalloproteins. In addition to measuring the *in vitro* antimicrobial properties of the present Ag(I) complexes their *in vivo* cytotoxicities were also examined using the insect model, *Galleria mellonella*.

Experimental

Infrared spectra were recorded in the region 4000–370 cm^{-1} on a Perkin Elmer System 2000 FT spectrometer. Microanalytical data were provided by the Microanalytical Laboratory, University College Dublin, Belfield, Dublin 4, Ireland. X-ray crystallographic data (Table 1) were collected at 150(2) K on a Bruker APEX II diffractometer and the structures were solved by direct methods and refined on F^2 using all the reflections.[36] All of the non-hydrogen atoms were refined using anisotropic atomic displacement parameters. Hydrogen atoms were inserted at

Table 1 Crystallographic data for complexes **3–7**

Complex	3	4	5	6	7
Formula	C$_{23.30}$H$_{20.3}$Ag N$_{5.3}$O$_2$	C$_{104}$H$_{78}$Ag$_6$N$_8$O$_{14}$	C$_{106}$H$_{78}$Ag$_6$N$_8$O$_{12}$	C$_{118}$H$_{102}$Ag$_6$N$_8$O$_{12}$	C$_{21}$H$_{22}$AgN$_3$O$_3$
Formula weight	514.42	2310.96	2302.98	2471.30	472.29
Crystal size, mm^3	0.33 × 0.22 × 0.21	0.23 × 0.15 × 0.12	0.43 × 0.32 × 0.06	0.32 × 0.19 × 0.12	0.20 × 0.17 × 0.07
Crystal system	Monoclinic	Orthorhombic	Triclinic	Triclinic	Orthorhombic
Space group	$P2_1/n$	$Pbcn$	$P\bar{1}$	$P\bar{1}$	$Pbca$
a, Å	9.7905(5)	20.6935(8)	11.7251(17)	17.6333(7)	9.6450(6)
b, Å	14.2012(7)	18.2786(7)	17.908(3)	19.3853(8)	19.0589(11)
c, Å	16.3251(9)	23.6859(10)	23.464(3)	30.4753(13)	21.2920(12)
α, °	90	90	111.403(2)	96.019(1)	90
β, °	101.864(1)	90	90.095(2)	95.831(1)	90
γ, °	90	90	101.710(2)	90.237(1)	90
V, Å^3	2221.3(2)	8959.1(6)	4476.2(11)	10 305.1(7)	3914.0(4)
Z	4	4	2	4	8
D_c, Mg m^{-3}	1.538	1.713	1.709	1.593	1.603
μ, mm^{-1}	0.938	1.358	1.357	1.185	1.057
Refl collected	19 005	80 667	35 083	89 958	37 907
Refl unique (R_{int})	4361 (0.0326)	9793 (0.0580)	15 686(0.0421)	40 407(0.0422)	4890 (0.0398)
Data/restraints/parameters	4361/23/326	9793/0/599	15 686/0/1194	40 407/ 3021/2665	4890/6/265
Goodness-of-fit on F^2	1.049	1.025	1.049	1.067	1.027
R_1, wR_2 [$I > 2\sigma(I)$]	0.0347, 0.0730	0.0316, 0.0695	0.0666, 0.1746	0.0505, 0.1130	0.0280, 0.0665
R_1, wR_2 (all data)	0.0460, 0.0782	0.0475, 0.0765	0.0856 0.1882	0.0739, 0.1228	0.0410, 0.0723
$\Delta\rho_{min}$, $\Delta\rho_{max}$, e Å^{-3}	0.936, −1.192	0.487, −0.788	4.988, −1.066	1.703, −0.978	0.447, −0.546

calculated positions using a riding model, except for those bonded to oxygen or nitrogen in complex **7**, which were located from difference maps and the coordinates refined. When the refinement for complex **5** had converged there remained a number of peaks in the electron density map at *ca.* 5 e Å^{-3}, and a second crystal showed the same effect. The geometry of these peaks was similar to the arrangement of silver ions in the main components, and it seems likely that these effects are due to a small twin contribution. However, attempts to incorporate this did not improve the model. In complex **6** there are two independent {[Ag(1-Bu-imid)$_2$]$_2$[Ag$_4$(9-aca)$_6$]} assemblies in the asymmetric unit, oriented about 90° to each other and very similar to one another. There is a disorder in the alkyl substituents attached to four of the eight imidazole groups and these were each modelled with partial occupancy of two overlapping sites (50 : 50 or 60 : 40). Some restraints (SAME and ISOR) were also employed.

Sterilisation of microbiological equipment and media was carried out at 394 K and 124 kPa for 20 min. Solutions that were susceptible to decomposition during autoclaving were sterilised by membrane filtration using 0.45 μm Millipore membrane filters. All worktops and benches were sterilised by washing with 70% (v/v) ethanol–water prior to use. Round-bottomed microtitre plates were read using a Labsystems iEMS Reader MF at 540 nm (*C. albicans*). Flat-bottomed microtitre plates were read using a Bio-Tek Synergy HT plate reader at 600 nm (*E. coli* and MRSA). Fungal cell density was measured using a Neubauer hemocytometer under a light microscope at a magnification of ×400. Bacterial cell density was recorded at an optical density of 600 nm using an Eppendorf Biophotometer.

Chemicals were purchased from commercial sources and were used without further purification. All of the silver(I) complexes were synthesised in the absence of light and the products were stored in the dark. [Ag$_4$(9-aca)$_4$(NH$_3$)$_2$] (**2**) was prepared from [Ag$_2$(9-aca)$_2$] (**1**) in accordance with the literature method.[35] *C. albicans* ATCC 10231 was obtained from the American Type Culture Collection, Manassas, VA, USA. *E. coli* was supplied as a clinical isolate by the Clinical Microbiology Laboratory, St. James's Hospital, Dublin, Ireland, and was originally isolated from a wound infection. MRSA was obtained as a clinical isolate from Microbiologics, North St. Cloud Mn, USA, and was originally isolated from a wound infection. *G. mellonella* larvae in the sixth developmental stage were obtained from Livefoods Direct Ltd., Sheffield, S25 4JJ, UK. They were stored at 288 K in wood shavings and used within 3 weeks of delivery. Significance of the larvae survival rates was analysed at 72 h using the log rank (Mantel–Cox) method utilising GraphPad Prism software (version 5). Three categories of significance were used (* = $p < 0.05$, ** = $p < 0.01$ and *** = $p < 0.001$).

Preparation of [Ag$_2$(9-aca)$_2$] (1)

This complex was prepared using an improved modification of the literature procedure.[35] 9-Anthracenecarboxylic acid (9-acaH) (1.117 g, 5.03 mmol) was added slowly to a solution of potassium hydroxide (0.282 g, 5.03 mmol) in water (30 cm^3) until pH 7 was reached. The solution was then filtered to remove any undissolved material. A solution of silver nitrate (0.849 g, 5.03 mmol) in water (10 cm^3) was added dropwise to the

K$^+$(9-aca)$^-$ solution. The resulting suspension was stirred for 0.5 h and then filtered. The yellow solid was washed with ethanol and air-dried. Yield: 1.202 g (73%).

Preparation of crystalline [Ag(imidH)$_{2.3}$(CH$_3$CN)$_{0.7}$](9-aca) (3)

[Ag$_2$(9-aca)$_2$] (**1**) (0.329 g, 0.5 mmol) was stirred in hot acetonitrile (70 cm^3) and any small traces of undissolved material was removed by filtration. Imidazole (0.207 g, 3.0 mmol) was dissolved in acetonitrile (10 cm^3) and added slowly to the stirred solution of **1**. The small amount of white precipitate which formed was filtered off and the clear filtrate was allowed to stand overnight. The white crystalline product which formed was filtered off, washed with acetonitrile and air-dried. Yield: 0.09 g (18%). Solubility: soluble in MeOH, hot EtOH and DMSO. Anal. calcd for C$_{23.30}$H$_{20.30}$AgN$_{5.30}$O$_2$: C, 54.40; H, 3.98; N, 14.43%. Found: C, 54.15; H, 3.91; N, 14.61%. IR (cm^{-1}, KBr): 3436, 3128, 3030, 2923, 2837, 2700, 2624, 2250, 1625, 1562, 1448, 1426, 1390, 1320, 1275, 1261, 1072.

Preparation of crystalline [Ag$_6$(imidH)$_4$(9-aca)$_6$(MeOH)$_2$] (4)

[Ag$_2$(9-aca)$_2$] (**1**) (0.109 g, 0.16 mmol) was suspended in methanol (10 cm^3) and to this was added a methanolic solution of imidazole (1 cm^3, 0.16 M, 0.16 mmol). The mixture was stirred for 1 h and then filtered. Diethyl ether was slowly added to the filtrate to precipitate the pale-yellow product. The solid was filtered off, washed with diethyl ether and air-dried. Crystals of the product formed in the ether filtrate. Yield: 0.04 g (44%). Solubility: soluble in MeOH and DMSO. Anal. calcd for C$_{104}$H$_{78}$Ag$_6$N$_8$O$_{14}$: C, 54.05; H, 3.40; N, 4.85%. Found: C, 53.75; H, 3.39; N, 4.73%. IR (cm^{-1}, KBr): 3448, 3045, 1625, 1538, 1484, 1433, 1393, 1320, 1273, 1238, 1178, 1090.

Preparation of crystalline {[Ag(1-Me-imid)$_2$]$_2$[Ag$_4$(9-aca)$_6$]} (5)

1-Methylimidazole (0.82 g, 1.0 mmol) was added to a hot suspension of [Ag$_2$(9-aca)$_2$] (**1**) (0.165 g, 0.25 mmol) in ethanol (30 cm^3) and the mixture immediately turned clear. Following filtration to remove any insoluble particles the filtrate was reduced to low volume by rotary evaporation. Diethyl ether was added to precipitate the beige solid, which was filtered off, washed with diethyl ether and allowed to air-dry. The solid was dissolved in DMSO and the solution reduced under high vacuum to yield the beige product. The solid was washed with a small amount of cold EtOH and air dried. The solid was again dissolved in the minimum volume of DMSO and crystals formed when the solution was allowed to stand for one week. Yield: 0.075 g (37%). Solubility: soluble in hot MeOH, EtOH and DMSO. Anal. calcd for C$_{106}$H$_{78}$Ag$_6$N$_8$O$_{12}$: C, 55.27; H, 3.42; N, 4.87%. Found: C, 54.98; H, 3.42; N, 4.63%. IR (cm^{-1}, KBr): 3468, 3116, 1621, 1565, 1536, 1428, 1392, 1321, 1275, 1235, 1180, 1112, 1087, 1017.

Preparation of crystalline {[Ag(1-Bu-imid)$_2$]$_2$[Ag$_4$(9-aca)$_6$]} (6)

[Ag$_2$(9-aca)$_2$] (**1**) (0.750 g, 1.14 mmol) was dissolved in hot acetonitrile (80 cm^3) and the solution filtered to remove any

traces of undissolved solid. The filtrate was allowed to cool to room temperature. 1-Butylimidazole (0.567 g, 4.56 mmol) was added and the resulting solution was stirred at room temperature for 20 h. After gravity filtration the filtrate was reduced to a low volume on a rotary evaporator and then diethyl ether was slowly added. The precipitated beige solid was filtered off, washed with diethyl ether and allowed to air-dry. The solid was recrystallised from hot ethanol to yield yellow crystals, which were then filtered off, washed with cold ethanol (1 cm^3) and allowed to air-dry. Yield: 0.301 g (51%). Solubility: soluble in MeOH, hot EtOH, CHCl$_3$ and DMSO. Anal. calcd for C$_{118}$H$_{102}$Ag$_6$N$_8$O$_{12}$: C, 57.35; H, 4.16; N, 4.53%. Found: C, 57.23; H, 4.23; N, 4.47%. IR (cm^{-1}, KBr): 3468, 2958, 1622, 1565, 1536, 1427, 1391, 1321, 1274, 1232, 1179, 1112, 1085, 1018.

Preparation of crystalline [Ag(apim)](9-aca)·H$_2$O (7)

[Ag$_2$(9-aca)$_2$] (1) (0.500 g, 0.76 mmol) was dissolved in hot acetonitrile (70 cm^3) and the solution filtered to remove any undissolved particles. 1-(3-Aminopropyl)imidazole (0.190 g, 1.52 mmol) was dissolved in acetonitrile (5 cm^3) and added to the stirred solution of 1. The resulting suspension was stirred for 0.5 h at room temperature and the beige solid was filtered off, washed with acetonitrile and air-dried. The solid was recrystallised from a 9 : 1 ethanol–methanol mixture to yield colourless crystals. Yield: 0.589 g (82%). Solubility: soluble in MeOH, hot EtOH and DMSO. Anal. calcd for C$_{21}$H$_{22}$AgN$_3$O$_3$: C, 53.40; H, 4.70%; N, 8.90%. Found: C, 53.31; H, 4.58%; N, 8.89%. IR (cm^{-1}, KBr): 3427, 3236, 3129, 3046, 2932, 1568, 1518, 1425, 1389, 1319, 1277, 1231, 1112, 1089, 1055.

In vitro antimicrobial screening. Minimal growth media (MM) was prepared as previously described.[35] Yeast extract peptone dextrose (YEPD) media was composed of 2% (w/v) glucose, 2% (w/v) bacteriological peptone and 1% (w/v) yeast extract. To solidify the media 2% (w/v) bacteriological agar was added when required. Nutrient broth and phosphate buffered saline (PBS) were made up according to the manufacturer's instructions (Scharlau Microbiology and Aldrich, respectively).

In vitro bacterial susceptibility testing. E. coli and methicillin-resistant S. aureus (MRSA) were grown on nutrient broth agar plates at 310 K and maintained at 277 K for short-term storage. All assays were run in triplicate and on three independent occasions. Fresh solutions of complexes were prepared immediately prior to testing. Complexes (0.020 g) were added to DMSO (1 cm^3) then water (9 cm^3) was added to give a stock solution (concentration 2000 mg cm^{-3}). Complexes with low solubility were tested as fine suspensions. The stock solution (1 cm^3) was added to water (9 cm^3) to yield a solution/suspension with a concentration of 200 μg cm^{-3}.

Nutrient broth (100 μl) was added to each well of a 96-well, flat-bottomed microtitre plate. Water (100 μl) was added to column 1 of the plate (negative control with no bacterial cells). Column 2 was the positive control (media with bacterial cells). 100 μl of the above complex solution (200 μg cm^{-3}) was added to every well in column 3. Serial dilutions (1 : 1) were made from column 3–12 to produce a test concentration range of 100–0.2 μg cm^{-3}.

E. coli and MRSA were grown overnight to the stationary phase in nutrient broth at 310 K and 200 rpm. The cells were diluted to give an optical density of 0.1 at λ = 600 nm. The cell suspension (100 μl) was added to every well in columns 2–12. The completed plates were incubated at 310 K in a static incubator and the final optical density recorded. MIC$_{50}$ values (minimum concentration required to inhibit 50% of cell growth) were then determined and expressed in terms of μM concentration.

In vitro fungal susceptibility testing. C. albicans (ATCC 10231) was grown on YEPD agar plates at 310 K and maintained at 277 K for short-term storage. All assays were run in triplicate and on three independent occasions. Fresh solutions of complexes were prepared immediately prior to testing. Complexes (0.020 g) were dissolved in DMSO (1 cm^3) and added to water (9 cm^3) to give a stock solution (concentration 2000 mg cm^{-3}). Complexes with low solubility were tested as fine suspensions. The stock solution (or suspension) (0.5 cm^3) was added to water (9.5 cm^3) to give a solution with a concentration of 100 μg cm^{-3}. MM (100 μl) was added to each well of a 96-well, round-bottomed microtitre plate. Water (100 μl) was added to column 1 of the plate (negative control, media with no fungal cells). Column 2 was the positive control (media and fungal cells only). 100 μl of the above complex solution (100 μg cm^{-3}) was added to every well in column 3. Serial dilutions (1 : 1) were made from columns 3–12 to produce a test concentration range of 50–0.1 μg cm^{-3}.

C. albicans was grown to the stationary phase overnight at 310 K on YEPD media. The cells were washed with PBS solution and resuspended in MM at a density of 5 × 10^5 cells cm^{-3}. The cell suspension (100 μl) was added to every well in columns 2–12. The completed plate was then covered with acetate foil (Sarstedt) to prevent dehydration. The plate was incubated at 310 K with continuous shaking for 24 h. The optical density (λ = 540 nm) of each well was recorded at 1 h intervals. MIC$_{100}$ values were then determined and expressed in terms of μM concentration.

In vivo cytotoxicity studies using Galleria mellonella. Since the immune system of insects bears a number of strong structural and functional similarities to the innate immune system of mammals,[37,38] insects can be used to screen the in vivo effect of drugs without the necessity of mammalian testing. The larvae of the greater wax moth, G. mellonella, have been utilised successfully since 1982 for in vivo studies of the pathogenicity of bacteria and fungi.[39–43] With specific reference to C. albicans, the G. mellonella model has provided invaluable information from fungal virulence studies.[44–48] Furthermore, the curative effects of antifungal prescription drugs[49] and some silver(I) compounds[50] on C. albicans-infected G. mellonella have already been determined.

G. mellonella larvae in the sixth developmental stage were used to determine the in vivo cytotoxicity of ketoconazole, AgNO$_3$ and complexes 1–7. Ten healthy larvae, between 0.20–0.40 g in weight and with no cuticle discoloration, were used in each test. Fresh solutions of the test complexes were prepared immediately prior to testing. Test compounds (0.020 g) were dissolved in DMSO (1 cm^3) and added to water (9 cm^3) to

give a stock solution (concentration 2000 mg cm^{-3}). Test solutions were made from this stock solution. In cases of limited solubility the resulting suspensions were used for the tests. Each compound was tested at two concentrations; 100 μg cm^{-3} and twice their MIC$_{100}$ value (in μg cm^{-3}). The test solution (20 μl) was administered to the larvae by injection directly into the haemocoel through the last pro-leg. The base of the pro-leg can be opened by applying gentle pressure to the sides of the larvae and this aperture will re-seal after removal of the syringe without leaving a scar. Larvae were placed in sterile petri dishes and incubated at 303 K for 72 h. Larvae survival was monitored after this 72 h period. Death was assessed by the lack of movement in response to stimulus together with discoloration of the cuticle. Three controls were employed in all assays. The first consisted of untouched larvae maintained at the same temperature as the test larvae. The second was larvae with the pro-leg pierced with an inoculation needle but no substance injected into them. The third control was larvae that were inoculated with 20 μl of the same sterile water used to make the test solutions.

In vivo antifungal screening using *G. mellonella.* *G. mellonella* larvae in the sixth developmental stage were used to determine the *in vivo* antimicrobial activity of ketoconazole, AgNO$_3$ and complexes **1–7**. As with the cytotoxicity studies (see above) ten larvae were injected with a fresh solution (or suspension) of the complex. Test concentrations were again 100 μg cm^{-3} and twice their MIC$_{100}$ value (in μg cm^{-3}). *C. albicans* was grown to the stationary phase in YEPD media at 310 K for 24 h. The cell concentration was assessed using a haemocytometer following dilution of the culture with PBS. The cells were washed three times with PBS and re-suspended in sterile PBS following harvesting by centrifugation (4000 × *g* for 10 min) to yield a suspension of 1 × 10^8 cell cm^{-3}.

Two treatments (prophylactic and treatment of infection) were employed in the screening of the test solutions. Five controls were used in each assay. The first control consisted of untouched larvae maintained at the same temperature as the test larvae (negative control). The second was larvae with the pro-leg pierced with an inoculation needle but no substance injected into them. The third control was larvae that were inoculated with the same sterile water (20 μl) used to make the test solutions, and the fourth was larvae inoculated with the same sterile PBS solution used to wash and make the *C. albicans* suspension. The positive control consisted of larvae inoculated with *C. albicans* and no test solution administered. The latter control is the one given in the results illustrated in Fig. 12. Significance was determined using the log rank (Mantel–Cox) method. Positive results were placed into one of three categories: * = *p* < 0.05, ** = *p* < 0.01 and *** = *p* < 0.001.

Prophylactic treatment. The test solution (20 μl) was administered to the larvae by injection as outlined above. Larvae were then placed in sterile petri dishes and incubated at 303 K for 1 h, after which time they were inoculated with 20 μl of the *C. albicans* cell suspension (2 × 10^6 cells). This number represents a lethal dose of fungal cells. The larvae were incubated at 303 K for 72 h and larvae survival was monitored immediately after this period.

Treatment of infection. Larvae were inoculated with 20 μl of the *C. albicans* suspension (2 × 10^6 cells) by injection as

described above. The larvae were then placed in sterile petri dishes and incubated at 303 K for 1 h, after which time the test solution (20 μl) was administered by injection. The larvae were incubated at 303 K for 72 h and larvae survival was monitored immediately after this period.

Results and discussion

Complex syntheses and structures

Synthetic routes to the complexes are given in Scheme 1. Our previously reported synthesis of [Ag$_2$(9-aca)$_2$] (**1**), from Ag$_2$O and 9-acaH,[35] had the major drawback of a low product yield (21%). A greatly improved yield (73%) was achieved by reacting the salt, K$^+$(9-aca)$^-$, with AgNO$_3$. The complex consists of polymeric ribbons of linked disilver(I), *syn–syn* bridged, dicarboxylate units and having an Ag–Ag distance of 2.851(1) Å.[35] Complex **1** was used as the starting material for the preparation of the other silver(I) complexes. The previously reported complex, [Ag$_4$(9-aca)$_4$(NH$_3$)$_2$] (**2**),[35] was prepared by reacting **1** with aqueous ammonia. Complex **2** was shown to be tetrameric and centrosymmetric, with two *syn–syn* bridging carboxylates linked to the bimetallic Ag–Ag core, and a further two, *syn–anti* bridged carboxylate ligands in the equatorial plane, being coordinated to one Ag in the bimetallic core and to a second Ag, with the latter also bonded to an NH$_3$ ligand. The closest Ag–Ag distance in the complex is 2.939(1) Å.

The imidazole complex, [Ag(imidH)$_{2.3}$(CH$_3$CN)$_{0.7}$](9-aca) (**3**), was synthesised from **1** and imidazole in acetonitrile. In this process, **1** disintegrates and re-assembles as a mononuclear complex where the metal ion is ligated by imidazole and acetonitrile, and the 9-aca$^-$ ligands are relegated to uncoordinated counterions. The X-ray crystal structure of **3** is shown in Fig. 2 and selected bond lengths and angles are given in Table 2. The Ag(I) ion forms short bonds to the imine N atom of two imidazole molcules (both Ag–N = 2.126(2) Å). These Ag–N bonds are slightly longer than those found in the mononuclear imidazole complexes, [Ag(imidH)$_2$]NO$_3$ (2.115(2) and 2.120(2) Å) and [Ag(imidH)$_2$]ClO$_4$ (2.131(2) Å),[51] and also in the trisilver(I) complex, [Ag$_3$(imidH)$_6$](ClO$_4$)$_3$ (2.075 Å).[52] A third ligand is coordinated to the metal in **3** and this has been modelled as a 70 : 30 disorder between acetonitrile and imidazole, respectively. The metal–nitrogen bonds to this third ligand are somewhat longer again (Ag1–N51 acetonitrile = 2.713(8) Å; Ag1–N41 imidazole = 2.588(17) Å). There is also a longer interaction with the carboxylate oxygen atom of a neighbouring 9-aca$^-$ unit (Ag1–O2B = 3.009(2) Å) (Fig. 3). In [Ag(imidH)$_{2.3}$(CH$_3$CN)$_{0.7}$]-
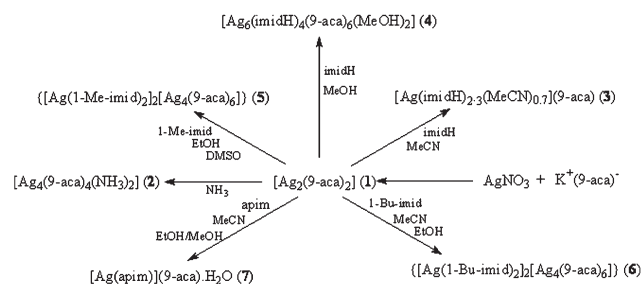
Scheme 1 Synthetic routes to the complexes.

Table 2   Selected bond lengths (Å) and angles (°)

Complex 3		N21–Ag1–N31	168.51(10)
Ag1–N21	2.126(2)	N21–Ag1–N41	96.1(6)
Ag1–N31	2.126(2)	N31–Ag1–N41	94.7(6)
Ag1–N41	2.588(17)	N21–Ag1–N51	93.7(3)
Ag1–N51	2.713(8)	N31–Ag1–N51	96.0(3)
Ag1–O2*	3.009(2)	N21–Ag1–O2*	93.98(8)
		N31–Ag1–O2*	92.38(7)
		N41–Ag1–O2*	76.5(3)
		N51–Ag1–O2*	88.78(18)

Symmetry transformations used to generate equivalent atoms:
* −x + 1/2, y − 1/2, −z + 1/2

Complex 4		N21–Ag1–N31	174.33(10)
Ag1–N21	2.088(2)	O(B–Ag2–O1A)	143.97(7)
Ag1–N31	2.089(2)	O1B–Ag2–O2A	154.09(7)
Ag1–Ag2	3.0651(4)	O1A–Ag2–O2A	54.34(7)
Ag2–O1B	2.218(2)	O1D–Ag3–O1C	162.45(8)
Ag2–O1A	2.416(2)	O1D–Ag3–O41	102.11(7)
Ag2–O2A	2.424(2)	O1C–Ag3–O41	92.58(8)
Ag3–O1D	2.1574(19)	O1D–Ag3–O2B	94.62(7)
Ag3–O1C	2.1681(19)	O1C–Ag3–O2B	95.22(7)
Ag3–O41	2.467(2)	O41–Ag3–O2B	88.95(7)
Ag3–Ag3	2.8818(5)		

Symmetry transformations used to generate equivalent atoms:
* −x, y, −z + 1/2

Complex 5		O12C*1–Ag1–O11C	156.3(2)
Ag1–O12C*	2.246(5)	O12C*–Ag1–O11A	100.7(2)
Ag1–O11C	2.272(5)	O11C–Ag1–O11A	103.0(2)
Ag1–O11A	2.316(6)	O12C*–Ag1–O11B	93.4(2)
Ag1–O11B	2.384(5)	O11C–Ag1–O11B	87.79(19)
Ag1–Ag1*	2.7860(12)	O11A–Ag1–O11B	88.2(2)
Ag1–Ag2*	2.9623(9)	O12B*–Ag2–O12A	140.4(2)
Ag1–Ag2	3.0079(9)	O11E–Ag3–O12E†	158.7(2)
Ag2–O12B*	2.188(5)	O11E–Ag3–O11F	99.5(2)
Ag2–O12A	2.193(5)	O12E†–Ag3–O11F	101.7(2)
Ag2–Ag1*	2.9623(9)	O11E–Ag3–O11D	94.7(2
Ag3–O11E	2.222(6)	O12E†–Ag3–O11D	88.4(2)
Ag3–O12E†	2.248(6)	O11F–Ag3–O11D	86.8(2)
Ag3–O11F	2.319(6)	O12D†–Ag4–O12F	140.9(2)
Ag3–O11D	2.389(6)	N1B–Ag5–N1A	170.8(3)
Ag3–Ag3†	2.7889(12)	N1B–Ag5–O11B	90.4(2)
Ag3–Ag4†	2.9489(9)	N1A–Ag5–O11B	96.1(2)
Ag3–Ag4	2.9838(9)	N1B–Ag5–O11A	100.9(3)
Ag4–O12D†	2.183(5)	N1A–Ag5–O11A	87.1(3)
Ag4–O12F	2.185(5)	O11B–Ag5–O11A	75.53(17)
Ag4–Ag3†	2.9488(9)	N1C–Ag6–N1D	171.2(3)
Ag5–N1B	2.124(9)	N1C–Ag6–O11D	91.8(2)
Ag5–N1A	2.136(8)	N1D–Ag6–O11D	95.4(2)
Ag6–N1C	2.131(8)	N1C–Ag6–O11F	84.1(3)
Ag6–N1D	2.134(8)	N1D–Ag6–O11F	102.8(3)
		O11D–Ag6–O11F	73.58(17)

Symmetry transformations used to generate equivalent atoms:
* −x + 1, −y, −z † −x + 2, −y, −z + 1

Complex 6		O1A–Ag1–O2D	132.81(16)
Ag1–O1A	2.207(4)	O1E–Ag2–O1F	154.83(15)
Ag1–O2D	2.217(4)	O1E–Ag2–O2A	108.55(15)
Ag1–Ag4	2.8750(6)	O1F–Ag2–O2A	91.25(14)
Ag1–Ag2	2.9028(6)	O1E–Ag2–O1B	94.95(15)
Ag2–O1E	2.222(4)	O1F–Ag2–O1B	99.15(16)
Ag2–O1F	2.226(4)	O2A–Ag2–O1B	93.86(14)
Ag2–O2A	2.335(4)	O1C–Ag3–O2B	135.29(16)
Ag2–O1B	2.357(4)	O1D–Ag4–O2C	89.46(15)
Ag2–Ag4	2.8365(5)	O1D–Ag4–O2F	107.09(18)
Ag2–Ag3	2.8770(6)	O2C–Ag4–O2F	93.00(15)
Ag3–O1C	2.174(4)	O1D–Ag4–O2E	92.01(17)
Ag3–O2B	2.192(4)	O2C–Ag4–O2E	102.37(15)
Ag3–Ag4	2.8949(6)	O2F–Ag4–O2E	155.64(13)
Ag4–O1D	2.275(4)	N1A–Ag5–N1B	176.98(18)
Ag4–O2C	2.304(4)	N1A–Ag5–O2A	93.44(16)
Ag4–O2F	2.354(4)	N1B–Ag5–O2A	89.43(15)
Ag4–O2E	2.355(4)	N1A–Ag5–O1B	89.53(16)
Ag5–N1A	2.116(5)		

Table 2   (Contd.)

Ag5–N1B	2.117(5)	N1B–Ag5–O1B	92.03(16)
Ag6–N1D	2.131(5)	O2A–Ag5–O1B	76.98(11)
Ag6–N1C	2.131(5)	N1D–Ag6–N1C	175.1(2)
		N1D–Ag6–O1D	90.55(19)
		N1C–Ag6–O1D	94.19(19)
		N1D–Ag6–O2C	97.24(17)
		N1C–Ag6–O2C	85.17(16)
		O1D–Ag6–O2C	73.86(12)
Ag7–O1G	2.196(4)	O1G–Ag7–O2J	132.37(16)
Ag7–O2J	2.202(4)	O2J–Ag7–O1L	105.68(16)
Ag7–O1L	2.564(4)	O1K–Ag8–O2L	153.12(15)
Ag7–Ag10	2.8760(6)	O1K–Ag8–O2G	99.71(16)
Ag7–Ag8	2.9646(6)	O2L–Ag8–O2G	104.46(16)
Ag8–O1K	2.217(4)	O1K–Ag8–O1H	104.54(16)
Ag8–O2L	2.257(4)	O2L–Ag8–O1H	85.64(14)
Ag8–O2G	2.301(4)	O2G–Ag8–O1H	93.64(14)
Ag8–O1H	2.382(4)	O1I–Ag9–O2H	135.17(16)
Ag8–Ag10	2.8165(5)	O2I–Ag10–O1J	88.66(15)
Ag8–Ag9	2.8544(6)	O2I–Ag10–O2K	95.31(16)
Ag9–O1I	2.178(4)	O1J–Ag10–O2K	109.95(17)
Ag9–O2H	2.203(4)	O2I–Ag10–O1L	99.16(15)
Ag9–Ag10	2.9511(6)	O1J–Ag10–O1L	87.68(16)
Ag10–O2I	2.286(4)	O2K–Ag10–O1L	157.45(14)
Ag10–O1J	2.304(4)	N1E–Ag11–N1F	176.84(19)
Ag10–O2K	2.309(4)	N1E–Ag11–O1H	93.65(16)
Ag10–O1L	2.374(4)	N1F–Ag11–O1H	89.24(16)
Ag11–N1E	2.112(5)	N1E–Ag11–O2G	87.63(17)
Ag11–N1F	2.113(5)	N1F–Ag11–O2G	94.29(16)
Ag12–N1H	2.122(5)	O1H–Ag11–O2G	76.30(11)
Ag12–N1G	2.124(5)	N1H–Ag12–N1G	175.0(2)
		N1H–Ag12–O1J	94.68(18)
		N1G–Ag12–O1J	90.14(18)
		N1H–Ag12–O2I	86.61(17)
		N1G–Ag12–O2I	95.99(18)
		O1J–Ag12–O2I	73.43(12)

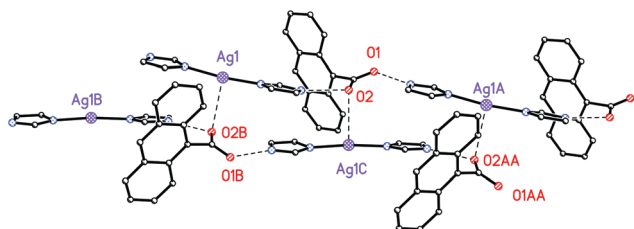| Complex 7			
Ag1–N1	2.0841(18)		
Ag1–N3*	2.1069(18)	N1–Ag1–N3*	177.76(7)

Symmetry transformations used to generate equivalent atoms:
* −x + 1/2, y + 1/2, z
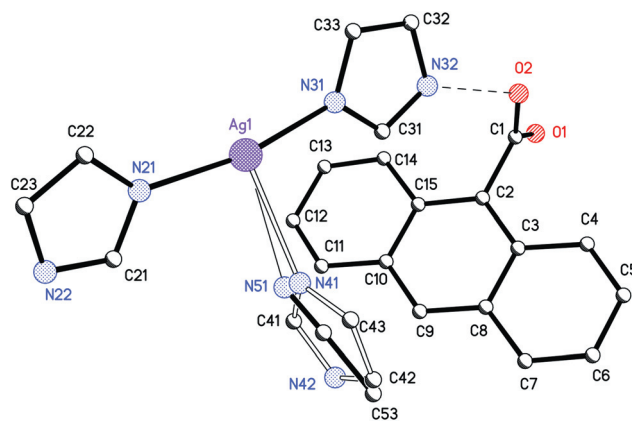
Fig. 2   The asymmetric unit of [Ag(imidH)$_{2.3}$(CH$_3$CN)$_{0.7}$](9-aca) (**3**) showing the disorder of one imidH with CH$_3$CN.

(9-aca) (**3**), the metal is coordinated approximately linearly with the first two imidazole ligands (N21–Ag1–N31 = 168.51(10)°), whilst the third ligand lies almost perpendicular (N21–Ag1–N51 = 93.7(3)°). The structure is linked into chains by hydrogen bonding between carboxylate oxygens and the hydrogen atoms on the pyrrole-type nitrogens (N–H) of the imidazoles (Fig. 3).

Table 3 Antimicrobial activities of complexes **1–7**, silver nitrate and the clinically used compounds, ketoconazole and silver sulfadiazine. MIC values are given in μM concentrations of complex and Ag(I) ions (in brackets)

Complex	E. coli MIC$_{50}$ (μM) {[Ag$^+$] μM}	MRSA MIC$_{50}$ (μM) {[Ag$^+$] μM}	C. albicans MIC$_{100}$ (μM) {[Ag$^+$] μM}
[Ag$_2$(9-aca)$_2$] (**1**)	22.44 {44.88}	11.36 {22.72}	0.95 {1.90}
[Ag$_4$(9-aca)$_4$(NH$_3$)$_2$] (**2**)	8.51 {34.04}	5.44 {21.76}	0.14 {0.56}
[Ag(imidH)$_{2.3}$(CH$_3$CN)$_{0.7}$](9-aca) (**3**)	20.66 {20.66}	67.07 {67.07}	0.38 {0.38}
[Ag$_6$(imidH)$_4$(9-aca)$_6$(MeOH)$_2$] (**4**)	1.87 {11.22}	5.85 {35.10}	0.54 {3.24}
{[Ag(1-Me-imid)$_2$]$_2$[Ag$_4$(9-aca)$_6$]} (**5**)	8.64 {51.84}	8.10 {48.60}	0.34 {2.04}
{[Ag(1-Bu-imid)$_2$]$_2$[Ag$_4$(9-aca)$_6$]} (**6**)	7.04 {42.24}	6.16 {36.96}	0.32 {1.92}
[Ag(apim)](9-aca)·H$_2$O (**7**)	30.13 {30.13}	27.50 {27.50}	0.43 {0.43}
AgNO$_3$	65.19 {65.19}	34.32 {34.32}	1.83 {1.83}
Ketoconazole			4.70
Silver sulfadiazine	73.05 {73.05}	50.20 {50.20}	

Fig. 3 Weak interactions of the silver(I) centre with the carboxylate oxygen atoms and the H-bonding between the imidazole N–H and carboxylate oxygens in [Ag(imidH)$_{2.3}$(CH$_3$CN)$_{0.7}$](9-aca) (**3**). The disordered solvate ligand has been omitted for clarity and H-bonds are represented by dashed lines.

This assembly is further supported by π–π stacking of the imidazole groups, with a centroid–centroid distance of 3.64 Å.

The IR spectrum of **3** exhibits a weak band at 2250 cm^{-1} for the C≡N bond stretching vibration. Bands are also observed at 3436 and 1072 cm^{-1}, corresponding to the N–H and C–N stretching vibrations of imidazole, respectively.[51] Bands for the anthracene ring system occur at 1625, 760 and 739 cm^{-1}.[53,54] Carboxylate $\nu_{(OCO)asym}$ and $\nu_{(OCO)sym}$ vibrations are present at 1562 and 1426 cm^{-1}, respectively, giving a $\Delta_{(OCO)}$ value of 136 cm^{-1}. This value indicates a bridging carboxylate which, in this case, is associated with the pseudo-bridging via hydrogen bonds.[55]

[Ag$_6$(imidH)$_4$(9-aca)$_6$(MeOH)$_2$] (**4**) was synthesised from **1** and imidazole in methanol, with a yield of 44%. Thus, a minor change in the reaction conditions (methanol as solvent as opposed to acetonitrile) causes a dramatic change in the product formulation. The X-ray crystal structure of the hexanuclear complex **4** (Fig. 4 and Table 2) shows that there is a two-fold axis through the molecule and that it contains both three- and five-coordinate silver(I) ions (Fig. 5). The Ag1–Ag2 bond length is 3.0651(4) Å, while the Ag3–Ag3A bond is significantly shorter at 2.8818(5) Å. Both of these Ag–Ag distances are close to that in metallic silver (2.889(6) Å) and are much shorter than the sum of the van der Waals radii of two Ag(0) atoms (3.44 Å), implying the existence of d^{10}–d^{10} interactions between two closed-shell Ag(I) ions. Such argentophilic interactions have been observed in a large number of multinuclear Ag(I) complexes.[56] In **4**, Ag1 is coordinated approximately linearly by two imidazoles (N21–Ag1–N31 bond angle of 174.33(10)°) with identical Ag–N bond lengths (2.088(2) Å). These latter bonds
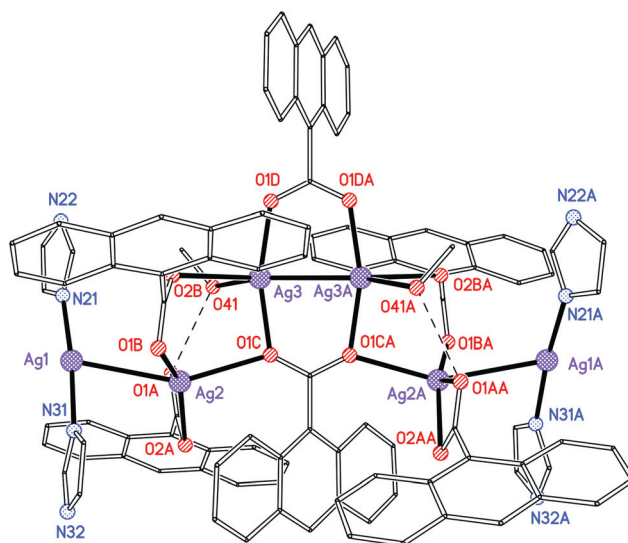
Fig. 4 Structure of [Ag$_6$(imidH)$_4$(9-aca)$_6$(MeOH)$_2$] (**4**). The two-fold axis lies in the plane of the page and bisects the Ag3–Ag3A vector (symmetry code −x,y,−z + 1/2). H-bonds are represented by dashed lines.
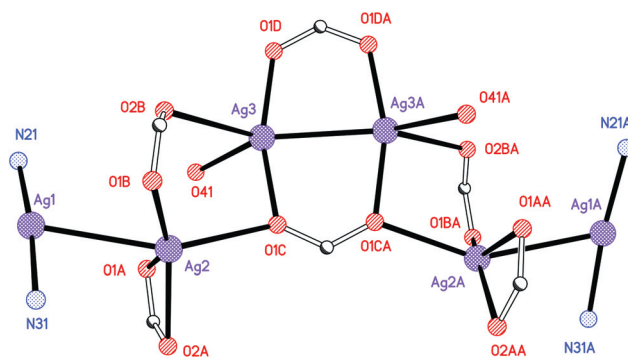
Fig. 5 Coordination sphere of [Ag$_6$(imidH)$_4$(9-aca)$_6$(MeOH)$_2$] (**4**) with the imidazole and anthracene rings omitted for clarity.

are slightly shorter than the corresponding Ag–N bond (2.126(2) Å) of the ordered imidazole in [Ag(imidH)$_{2.3}$(CH$_3$CN)$_{0.7}$](9-aca) (**3**). In complex (**4**), Ag2 is coordinated to three different carboxylate groups as well as being bonded to Ag1. Ag3 is also coordinated to three different carboxylate groups, plus the oxygen of a coordinated methanol molecule and another silver ion (Ag3A).

Two of the carboxylate ligands are in the *syn–syn* configuration (O1C and O1Ca, O1D and O1DA), two are *syn–anti* (O1B and O2B, O1BA and O2BA) and two are coordinated in a symmetrical, bidentate chelation mode (O1A and O2A, O1AA and O2AA). There is also intramolecular H-bonding between the OH of the alcohol group and a neighbouring carboxylate oxygen atom (O41–O1A 2.782(3) Å), as well as intermolecular H-bonding between the amine hydrogen of the imidazole and a carboxylate oxygen of a neighbouring 9-aca⁻ ligand (N22–O2A 2.796(3) Å under symmetry operation −x + 1/2, y − 1/2, z and N32–O2B, 2.815(3) under −x + 1/2, y + 1/2, z). A very weak π-interaction between Ag(1) and the anthracene ring of a neighbouring molecule is also observed. The structure of **4** is quite different to that of the recently reported, hexanuclear, centrosymmetric complex, [Ag$_6$(dmp)$_2$(9-aca)$_6$] (dmp = 2,6-dimethylpyridine),[57] prepared by reacting AgNO$_3$ with 9-acaH in the presence of dmp. In this complex, all six Ag(I) ions are ligated by carboxylate oxygen atoms, and the two heterocyclic, N-donor dmp ligands are bonded to separate metal centres. In addition, the solid state structure of [Ag$_6$(dmp)$_2$(9-aca)$_6$] exhibits intramolecular and intermolecular anthracene C–H···Ag interactions as well as π–π stacking interactions. The metal coordination geometry within the hexanuclear core of **4** is also very different to that recently reported for a number of hexa-Ag(I) thiosemicarbazone complexes and, furthermore, the shortest Ag–Ag distances in the latter complexes are significantly longer than in **4**.[57–59]
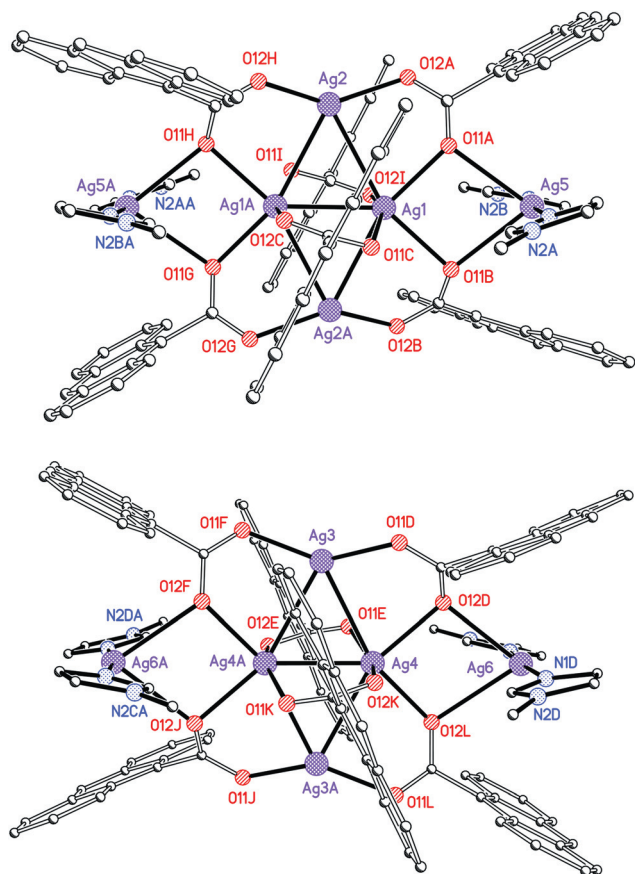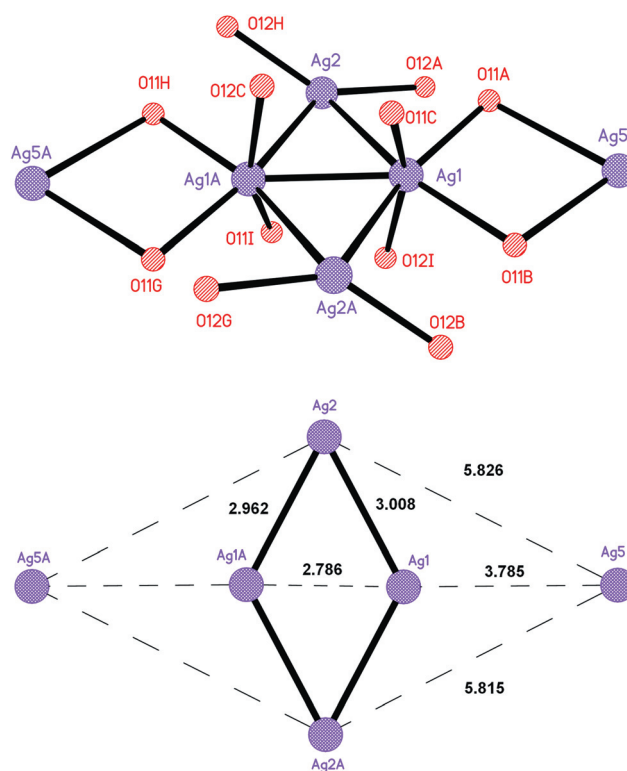
The IR spectrum of **4** has peaks at 3448 and 1091 cm⁻¹ for the O–H and C–N stretching vibrations of MeOH and imidazole, respectively. Distinctive bands for the vibrations of the anthracene ring system appear at 1625, 760 and 736 cm⁻¹. Carboxylate $\nu_{(OCO)asym}$ and $\nu_{(OCO)sym}$ vibrations occur at 1538 and 1433 cm⁻¹, respectively, giving a $\Delta_{(OCO)}$ value of 105 cm⁻¹ and implying the presence of bridging carboxylates.

The initial beige precipitate which formed upon reacting **1** with 1-methylimidazole (1-Me-imidH) in ethanol was recrystallised from DMSO to give {[Ag(1-Me-imid)$_2$]$_2$[Ag$_4$(9-aca)$_6$]} (**5**). The X-ray crystal structure of **5** (Fig. 6 and Table 2) shows it to consist of two independent, centrosymmetric molecules which differ chiefly in the angle between the planes of the anthracene ligands. Each molecule of **5** contains a dianionic, complex central core, [Ag$_4$(9-aca)$_6$]²⁻, with the two complex cations, [Ag(1-Me-imidH)$_2$]⁺, on the periphery of the molecule. It is the manner in which these two dications are each linked to the tetranuclear core by a bridging carboxylate oxygen atom that principally distinguishes this structure from **4**.

The central tetrasilver(I) cluster in **5** contains Ag–Ag bond lengths ranging from 2.786 to 3.009 Å, and the average distance from a core metal to a peripheral metal is 5.821 Å (Fig. 7). The Ag1–Ag1A distance of 2.786 Å in **5** is the shortest in the present family of Ag(I) anthracenecarboxylate complexes and it is also significantly smaller than any argentophilic interactions found in [Ag$_6$(dmp)$_2$(9-aca)$_6$] (minimum Ag–Ag is 2.895 Å).[57] In complex **5**, two 9-aca⁻ ligands (O11C, O12C and O11I, O12I) are coordinated in a *syn–syn* fashion to the central silver(I) ions (Ag1, Ag1A), and the other four carboxylate ligands are

Fig. 6 The two independent molecules of [Ag(1-Me-imid)$_2$]$_2$[Ag$_4$(9-aca)$_6$] (**5**) illustrating the difference in arrangement of the anthracene ligands.

Fig. 7 Simplified structures of [Ag(1-Me-imid)$_2$]$_2$[Ag$_4$(9-aca)$_6$] (**5**) showing (a) Ag–Ag and Ag–O bonding and (b) Ag–Ag bond distances (Å) for one of the molecules.
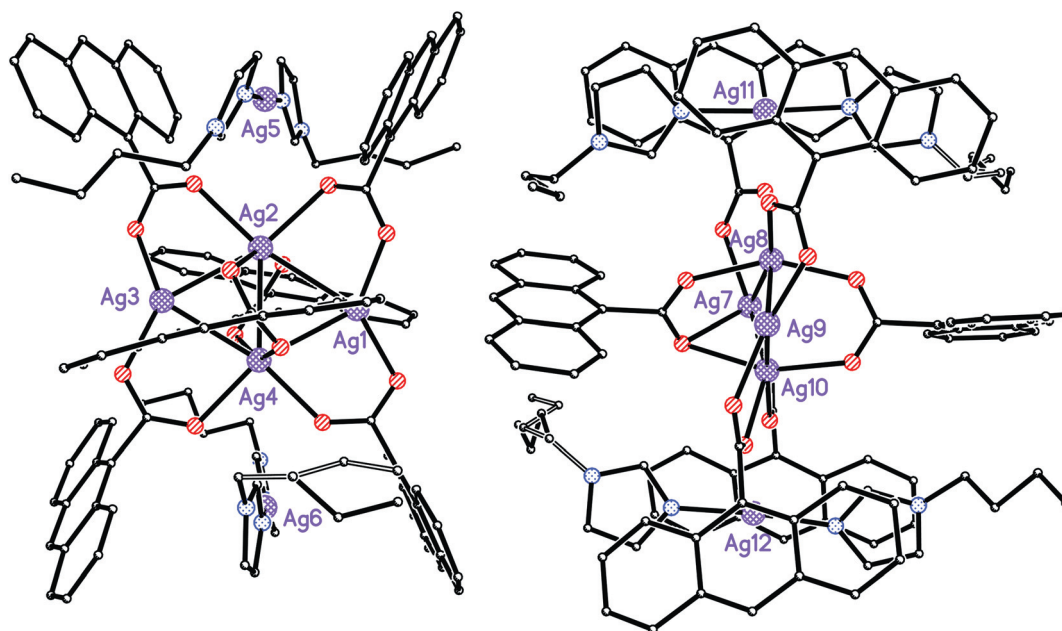
Fig. 8 X-ray crystal structure of [Ag(1-Bu-imid)$_2$]$_2$[Ag$_4$(9-aca)$_6$] (**6**) showing the two independent assemblies.

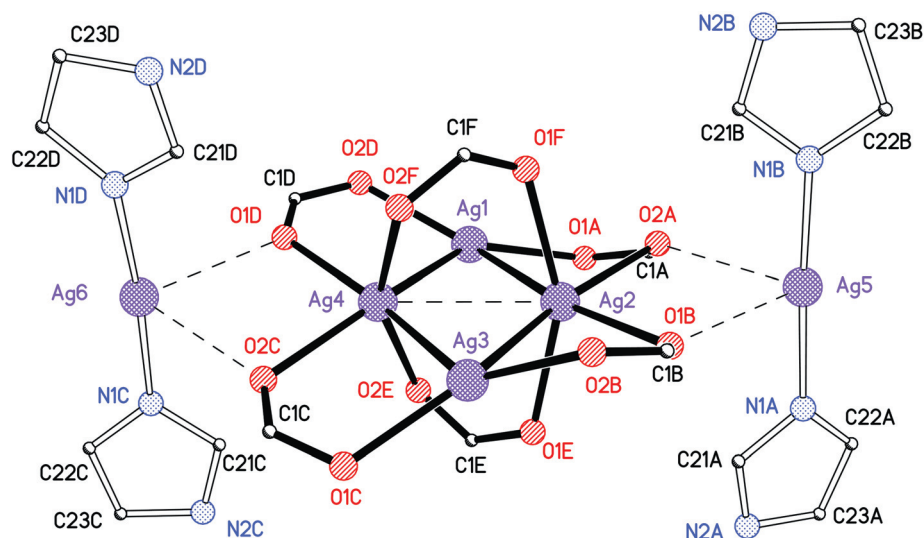**Fig. 9** Structure of one molecule of {[Ag(1-Bu-imid)$_2$]$_2$[Ag$_4$(9-aca)$_6$]} (**6**) with the anthracene rings and alkyl chains removed for clarity.

coordinated to two central silver(I) ions and one peripheral silver(I) ion. The average core Ag–O bond length is 2.304 Å (e.g. Ag1–O11) and the average peripheral Ag–O bond length is 2.671 Å (e.g. (Ag5–O11A). The 1-Me-imid ligands are coordinated to the metals through the imine N atom and lie in an approximately linear arrangement (N1A–Ag5–N1B bond angle is 171.10°). The methyl groups on each of the two imidazole ligands are *cis* to each other and are orientated towards the centre of the molecule.

The IR spectrum of **5** contains bands at 1621, 772 and 736 cm^{-1} for the anthracene ring system, and a band for the C–N stretching vibration of the imidazole ring at 1087 cm^{-1}. The carboxylate $\nu_{(OCO)asym}$ and $\nu_{(OCO)sym}$ stretching vibrations occur at 1565 and 1428 cm^{-1}, respectively, giving a $\Delta_{(OCO)}$ value of 137 cm^{-1}. This value indicates the presence of carboxylates with a chelating and/or bridging mode of coordination.

The reaction of **1** with 1-butylimidazole in acetonitrile produced a beige solid which, upon recrystallisation from ethanol, yielded {[Ag(1-Bu-imid)$_2$]$_2$[Ag$_4$(9-aca)$_6$]} (**6**). The X-ray crystal structure of **6** (Fig. 8, Table 2) shows two very similar but independent assemblies within the asymmetric unit and orientated at approximately 90° to each other. There is also some disorder within the butyl chains of the imidazole ligands. The complex contains two-, four- and six-coordinate silver(I) ions (Fig. 9). Two of the metals are coordinated approximately linearly to the imine nitrogen atoms of two 1-Bu-imid ligands (bond angles of 176.98(18), 175.1(2), 176.84(19) and 175.0(2)°), with an average Ag–N bond length of 2.124 Å. There are also longer
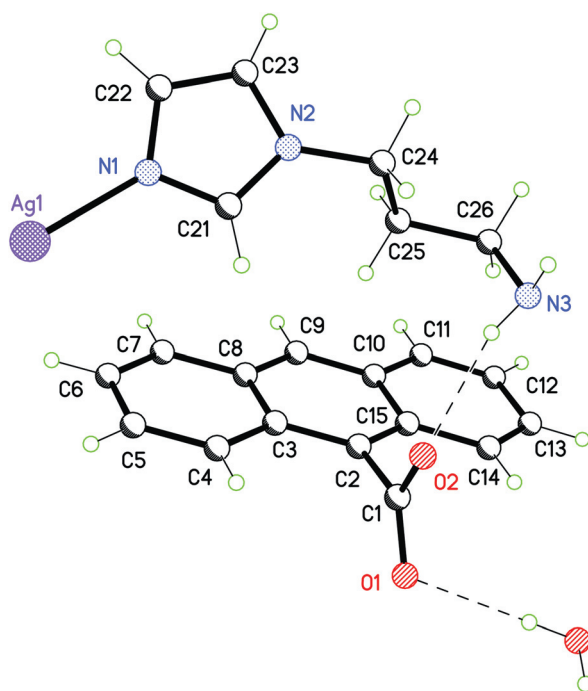
Fig. 10 Structure of one asymmetric unit of [Ag(apim)](9-aca)·H₂O (**7**).

interactions of these silver ions with carboxylate oxygen atoms at the central core of the molecule (Ag5–O2A, Ag5–O1B, Ag6–O2C and Ag6–O1D bond lengths of 2.696(4), 2.809(4), 2.756(4) and 2.603(4) Å, respectively). Within the central, dicationic $[Ag_4(9\text{-aca})_6]^{2-}$ core there are five Ag–Ag bonds, with lengths ranging from 2.8165(5) to 2.9646(6) Å. All of the anthracene ligands use both of their carboxylate oxygen atoms to coordinate to two different silver ions in a *syn–syn* binding mode. There are no intramolecular or intermolecular π–π interactions between either the anthracene or the imidazole rings. The structure of **6** is very similar to that of **5**, indicating that the change in the length of the alkyl chain (from methyl to butyl) on the tertiary N atom of the imidazole ring does not appear to affect the core structure of the product.

The IR spectrum of **6** contains bands for the anthracene rings at 1622, 759 and 732 cm^{-1}. The band representing the C–N stretching vibration of the 1-Bu-imid ligands occur at 1085 cm^{-1}. Carboxylate $\nu_{(OCO)asym}$ and $\nu_{(OCO)sym}$ vibrations appear at 1565 and 1427 cm^{-1}, respectively, giving a $\Delta_{(OCO)}$ value of 138 cm^{-1} and indicating that the carboxylate ligands are coordinated in either a chelating or a bridging mode.

[Ag(apim)](9-aca)·H₂O (**7**) was synthesised in high yield from **1** and 1-(3-aminopropyl)-imidazole (apim) in acetonitrile. The X-ray crystal structure of **7** (Fig. 10, Table 2) shows the metal bonded to the imine nitrogen atom of the imidazole ring (Ag1–N1 = 2.0841(18) Å). The metals and the apim ligands bond together to form 1-D, zig-zag polymeric chains (Fig. 11) with the silver being coordinated approximately linearly to the imine nitrogen of one apim and the nitrogen of the pendant amine function of another imidazole (Ag1–N3A = 2.1069(18) Å and N1–Ag1–N3A = 177.76(7)°). π–π Stacking interactions are also observed between the imidazole rings, creating 2-D sheets (ESI† Fig. a). The water molecule of hydration links to the anionic

9-aca⁻ units through H-bonds forming polymeric chains which zig-zag in-and-out through the spaces in the $[Ag(apim)]_n^{n+}$ sheets (ESI† Fig. b). There are also H-bonding interactions linking a carboxylate oxygen to the hydrogen of the pendant amine group (ESI† Fig. c). Due to the relatively long distance between the sheets, there are no π–π interactions involving the anthracene rings. The structurally similar and previously characterised[60] apim complex, [Ag(apim)]ClO₄, also shows the same type of zig-zag arrangement of polymeric $[Ag(apim)]_n^{n+}$ chains, but this complex has weak metal–anion (ClO₄⁻) interactions which are not present in **7**.

The IR spectrum of **7** contains bands at 3427 and 3236 cm^{-1} corresponding to the apim NH₂ stretching vibrations, and a band at 1089 cm^{-1} for the C–N stretching vibration of the imidazole ring. Two bands are present at 761 and 735 cm^{-1} for the stretching vibrations of the anthracene ring system, but the third band, which is usually located at approximately 1625 cm^{-1}, is masked by the strong $\nu_{(OCO)asym}$ carboxylate stretching band centred at 1568 cm^{-1}. The $\nu_{(OCO)sym}$ stretching vibration occurs at 1426 cm^{-1}, thus giving a $\Delta_{(OCO)}$ value of 142 cm^{-1}. Although this value implies that the carboxylate is either chelating or bridging[55] it is evident from the X-ray crystal structure of the complex that this is not the case. Thus, it must be stressed that coordination mode assignments based on $\Delta_{(OCO)}$ values[55] can, indeed, be quite tentative.

In summary, it is evident from the formulations of complexes **3–7** that a slight change in either the reaction solvent or the structure of the imidazole ligand employed during the synthesis can have a marked effect on the structure of the isolated product. Unsubstituted imidazole leads to the mononuclear species, **3**. Having an alkyl substituent on the tertiary N atom of the imidazole gives the hexanuclear complexes, **4**, **5** and **6**. When the alkyl substituent carries an amine functionality on its terminus the polymeric complex **7** forms.

Antimicrobial activity

The silver(I) complexes, **1–7**, the simple silver(I) salt, silver nitrate, and selected, known antimicrobial drugs (antibacterial silver sulfadiazine and antifungal ketoconazole) were screened, *in vitro*, for their ability to inhibit the growth of pathogenic bacterial and fungal cells. Activities (as MIC$_{50}$ or MIC$_{100}$ values) are reported (Table 3) as μM concentrations of the complexes and also as μM concentrations of administered Ag(I) ion in consideration of the different amounts of Ag(I) ions present in the various complexes. Test solutions (or suspensions) were made by dissolving the sample in DMSO and diluting with water to yield the required concentration. The maximum DMSO concentration in any test solution was 0.5% v/v, and at this level the DMSO does not inhibit the growth of the microbial cells. The metal-free ligands (9-acaH and the various imidazoles) were also screened for their biological activity and all were inactive at a concentration of ≤100 μg cm^{-3}.

In terms of both complex concentration and the concentration of Ag(I) ions, **1–7** were all more active than AgNO₃ and silver sulfadiazine against Gram-negative *E. coli*. Against Gram-positive MRSA, only **3** was less active, in terms of complex concentration, than AgNO₃. Comparisons made on the basis of Ag(I) ion concentration reveal that only complexes **1**, **2** and **7** were
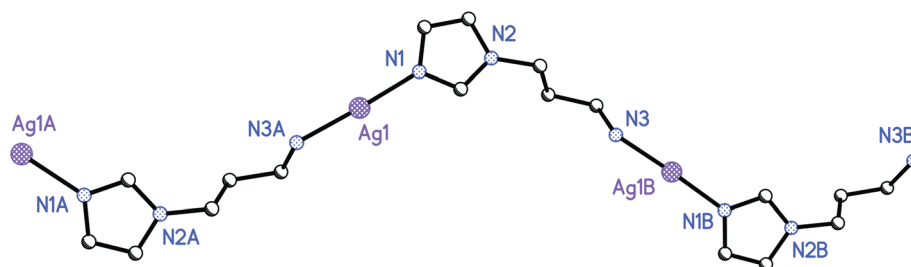
Fig. 11 $[Ag(apim)]_n{}^{n+}$ cationic polymer chains in the structure of $[Ag(apim)](9\text{-aca})\cdot H_2O$ (**7**).

more active against MRSA than $AgNO_3$. In terms of Ag(I) ion concentration, **1**, **2** and **7** were more active than $AgNO_3$ against both species of bacteria. The structurally similar double complex salts, **5** and **6**, displayed similar antibacterial properties.

With respect to complex concentrations, **1**–**7** were all considerably more active against *C. albicans* than both ketoconazole and $AgNO_3$ (Table 3). However, as a function of Ag(I) ion concentration, only **2**, **3** and **7** were a lot more active than $AgNO_3$. The latter three complexes, which all contain N-donor imidazole ligands, were more active than the parent carboxylate complex, **1**. Complexes **5** and **6**, which contain imidazole ligands carrying substituents (Me or Bu) on the N1 atom of the heterocyclic ring, and which also have ligated 9-aca⁻ anions, appear to be only marginally more active than hexanuclear **4**, which has un-substituted imidazoles coordinated to two of the metal centres. Against all three microbial species, and in terms of Ag(I) ion content, only **2** and **7** were significantly more active than $AgNO_3$.

In vivo toxicity profiling was carried out using the *G. mellonella* insect model. *G. mellonella* larvae were administered with test solutions (or suspensions) by injection directly into the haemocoel through the last pro-leg. Survival was monitored after 72 h and death was assessed by the lack of movement in response to stimulus together with discoloration of the cuticle. The toxicity of all of the test samples was assessed at two different concentrations: 100 µg cm⁻³ and twice their MIC_{100} value. Silver nitrate and ketoconazole were used as reference standards. It was found that all of the larvae survived the highest administered concentration (100 µg cm⁻³) of $AgNO_3$, ketoconazole and complexes **1**–**7**. Two types of *in vivo* antifungal screening protocols were conducted using the larvae: (i) prophylactic treatment and (ii) the treatment of infection (pre-infected larvae). The larvae were infected with a lethal dose of *C. albicans* (2×10^6 fungal cells) in each of the two screening protocols. For prophylactic treatment, the test compound was administered 1 h prior to infection with *C. albicans* cells, while for the treatment of infection experiments the compound was administered 1 h after infection with *C. albicans*. In each case, larvae survival was assessed after a 72 h interval and the results are presented in Fig. 12.

Complex **2**, administered prophylactically at a concentration of 100 µg cm⁻³, significantly increased the survival rate (90%) of *G. mellonella* larvae 72 h after infection with a lethal dose of *C. albicans* cells. This response was superior to that given by $AgNO_3$ (80%) and ketoconazole (75%), which were, in turn, better than that the other Ag(I) complexes. When the prophylactic experiment was repeated using a concentration dosage of $2 \times MIC_{100}$ concentration the % survival of larvae decreased in all cases. Complex **2** still offered the best protection (65%
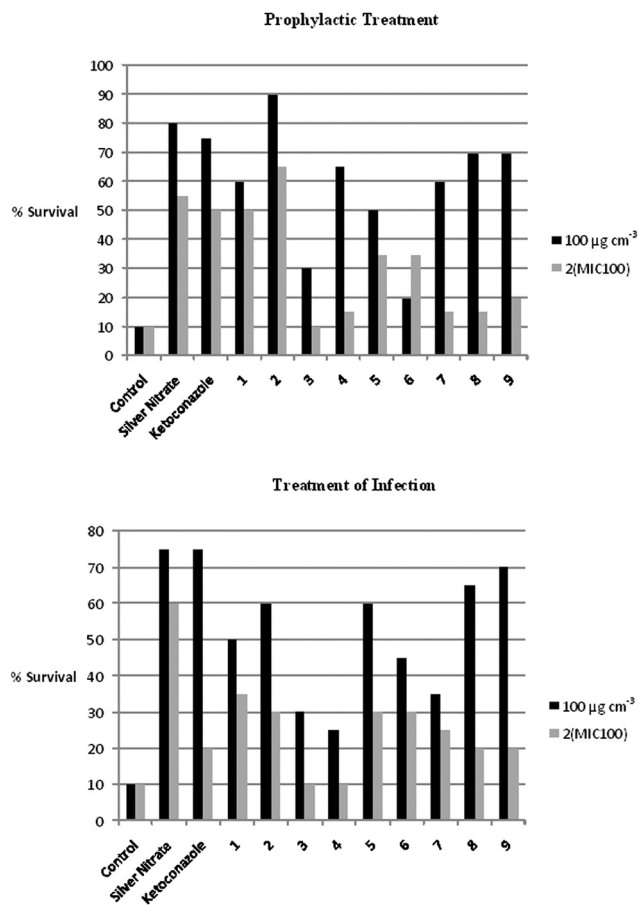

Fig. 12 Survival of *G. mellonella* larvae 72 h after being infected with a lethal dose of *C. albicans* (2×10^6 fungal cells). For prophylactic treatment, the test compound was administered 1 h prior to infection with *C. albicans* cells, while for the treatment of infection experiments the compound was administered 1 h after infection with *C. albicans*. Compounds tested were $AgNO_3$, ketoconazole and **1**–**7**. All compounds were administered at two different concentrations (100 µg cm⁻³ and $2 \times MIC_{100}$ concentration in µg cm⁻³).

survival) and this was followed by $AgNO_3$ (55%). Complex **1** and ketoconazole were equally active (50%) at this dosage.

Larvae which were pre-infected with a lethal dose of *C. albicans* cells and then subsequently treated with 100 µg cm⁻³ of the test compounds, responded best to ketoconazole and silver nitrate (both gave 75% survival after 72 h). The most effective Ag(I) complex was **7** (70%), followed by **5** (60%) and **2** (60%). At the $2 \times MIC_{100}$ concentration dosage all of the test materials

generally offered less protection towards a pre-existing fungal infection than at the 100 μg cm^{-3} concentration level. AgNO$_3$ performed best (60% survival), followed by **1** (35%), **2** (30%) and **5** (30%). Under the same conditions, only 20% of infected larvae survived upon treatment with ketoconazole.

In summary, the prophylactic method of administering the silver(I) complexes proved more effective at increasing the survival rate of *G. mellonella* infected with *C. albicans*. This may be attributed not only to the efficacy of the test compound (direct anti-effect) but also to the anticipated increase in the number of haemocytes, antimicrobial peptides and proteins produced by the innate immune system of the insect in response to the presence of the administered foreign substance (indirect anti-effect).[50]

Conclusions

A myriad of structurally diverse Ag(I) complexes containing the 9-anthracenecarboxylate anion and imidazoles can be synthesised from the parent complex, [Ag$_2$(9-aca)$_2$] (**1**). While many of the complexes possess excellent, *in vitro* antifungal and antibacterial activities they are, unanimously, more effective against fungal cells. *G. mellonella* can survive high doses of the Ag(I) complexes administered *in vivo*, and a number of the complexes offer significant protection to larvae infected with a lethal dose of pathogenic *C. albicans* cells. These silver complexes offer significant potential as new antimicrobial agents for clinical application.

Acknowledgements

Notes and references

1 S. R. Wilkinson and J. M. Kelly, *Expert Rev. Mol. Med.*, 2009, **11**, e31.
2 H. S. Fraimow and C. Tsigrelis, *Crit. Care Clin.*, 2011, **27**, 163.
3 M. H. Miceli, J. A. Díaz and S. A. Lee, *Lancet Infect. Dis.*, 2011, **11**, 142.
4 A. Melaiye and W. J. Youngs, *Expert Opin. Ther. Pat.*, 2005, **15**, 125.
5 S. Silver, *FEMS Microbiol. Rev.*, 2003, **27**, 341.
6 A. B. G. Lansdown, *Crit. Rev. Toxicol.*, 2007, **37**, 237.
7 M. K. Dasgupta, *Adv. Perit. Dial.*, 1994, **10**, 195.
8 A. P. Adams, E. M. Santschi and M. A. Mellencamp, *Vet. Surg.*, 1999, **28**, 219.
9 W. W. Monafo and B. Freedman, *Surg. Clin. North Am.*, 1987, **67**, 133.
10 J. B. Wright, K. Lam and R. E. Burrell, *Am. J. Infect. Control*, 1998, **26**, 572.
11 J. B. Wright, K. Lam, J. Hansen and R. E. Burrell, *Am. J. Infect. Control*, 1999, **27**, 344.
12 J. Jain, S. Arora, J. M. Rajwade, P. Omray, S. Khandelwal and K. M. Paknikar, *Mol. Pharmaceutics*, 2009, **6**, 1388.
13 D. R. Monteiro, L. F. Gorup, A. S. Takamiya, A. C. Ruvollo-Filho, E. Rodrigues de Camargo and D. Barros Barbosa, *Int. J. Antimicrob. Agents*, 2009, **34**, 103.
14 M. McCann, M. Geraghty, M. Devereux, D. O'Shea, J. Mason and L. O'Sullivan, *Met.-Based Drugs*, 2000, **7**, 185.
15 B. Coyle, K. Kavanagh, M. McCann, M. Devereux and M. Geraghty, *BioMetals*, 2003, **16**, 321.
16 B. Coyle, P. Kinsella, M. McCann, M. Devereux, R. O'Connor, M. Clynes and K. Kavanagh, *Toxicol. in Vitro*, 2004, **18**, 63.
17 R. Rowan, M. McCann and K. Kavanagh, *Med. Mycol.*, 2010, **48**, 498.
18 S. J. Berners-Price, R. K. Johnson, A. J. Giovenella, L. F. Faucette, C. K. Mirabelli and P. J. Sadler, *J. Inorg. Biochem.*, 1988, **33**, 285.
19 K. M. Hindi, A. J. Ditto, M. J. Panzner, D. A. Medvetz, D. S. Han, C. E. Hovis, J. K. Hilliard, J. B. Taylor, Y. H. Yun, C L. Cannon and W. J. Youngs, *Biomaterials*, 2009, **30**, 3771.
20 M.-X. Li, D. Zhang, L.-Z. Zhang and J.-Y. Niu, *Inorg. Chem. Commun.*, 2010, **13**, 1268.
21 M. Devereux, M. McCann, D. O' Shea, R. Kelly, D. A. Egan, C. Deegan, K. Kavanagh, V. McKee and G. J. Finn, *J. Inorg. Biochem.*, 2004, **98**, 1023.
22 M. McCann, B. Coyle, S. McKay, P. McCormack, K. Kavanagh, M. Devereux, V. McKee, P. Kinsella, R. O'Connor and M. Clynes, *BioMetals*, 2004, **17**, 635.
23 B. Coyle, M. McCann, K. Kavanagh, M. Devereux, V. McKee, N. Kayal, D. A. Egan, C. Deegan and G. J. Finn, *J. Inorg. Biochem.*, 2004, **98**, 1361.
24 K. B. Holt and A. J. Bard, *Biochemistry*, 2005, **44**, 13214.
25 H. Wang, N. Law, G. Pearson, B. E. Van Donegan, R. M. Jarvis, R. Goodacre and J. R. Lloyd, *J. Bacteriol.*, 2009, **192**, 1143.
26 Q. Feng, *J. Biomed. Mater. Res.*, 2000, **52**, 662.
27 W.-K. Jung, H.-C. Koo, K.-W. Kim, S. Shin, S.-H. Kim and Y.-H. Park, *Appl. Environ. Microbiol.*, 2008, **74**, 2171.
28 S. L. Percival, P. G. Bowler and D. Russell, *J. Hosp. Infect.*, 2005, **60**, 1.
29 S. Y. Liau, D. C. Read, W. J. Pugh, J. R. Furr and A. D. Russell, *Lett. Appl. Microbiol.*, 1997, **25**, 279.
30 G. McDonnel and A. D. Russell, *Clin. Microbiol. Rev.*, 1999, **12**, 147.
31 A. D. Russell and W. B. Hugo, *Prog. Med. Chem.*, 1994, **31**, 351.
32 H. Arkawa and J. F. Neault, *Biophys. J.*, 2001, **81**, 1580.
33 H.-J. Park, J. Y. Kim, J. Kim, J.-H. Lee, J.-S. Hahn, M. B. Gu and J. Yoon, *Water Res.*, 2009, **43**, 1027.
34 H. Le Pape, F. Solano-Serena, P. Contini, C. Devillers, A. Maftah and P. Leprat, *J. Inorg. Biochem.*, 2004, **98**, 1054.
35 R. Curran, J. Lenehan, M. McCann, K. Kavanagh, M. Devereux, D. A. Egan, G. Clifford, K. Keane, B. S. Creaven and V. McKee, *Inorg. Chem. Commun.*, 2007, **10**, 1149.
36 G. M. Sheldrick, *Acta Crystallogr., Sect. A: Found. Crystallogr.*, 2007, **64**, 112.
37 J. Klein, *Scand. J. Immunol.*, 1997, **46**, 558.
38 M. Salzet, *Trends Immunol.*, 2001, **22**, 285.
39 J. B. Walters and N. A. Ratcliffe, *J. Insect Physiol.*, 1983, **29**, 417.
40 G. Dunphy and A. Halwani, *J. Insect Physiol.*, 1997, **43**, 1023.
41 G. B. Dunphy, D. B. Morton, A. Kropinski and J. M. Chadwick, *J. Invertebr. Pathol.*, 1986, **47**, 48.
42 K. Kavanagh and E. P. Reeves, *FEMS Microbiol. Rev.*, 2004, **28**, 101.
43 J. Renwick, P. Daly, E. P. Reeves and K. Kavanagh, *Mycopathologia*, 2006, **161**, 377.
44 M. Brennan, D. Y. Thomas, M. Whiteway and K. Kavanagh, *FEMS Immunol. Med. Microbiol.*, 2002, **34**, 153.
45 D. Bergin, L. Murphy, J. Keenan, M. Clynes and K. Kavanagh, *Microbes Infect.*, 2006, **8**, 2105.
46 D. Bergin, E. P. Reeves, J. Renwick, F. B. Wientjes and K. Kavanagh, *Infect. Immun.*, 2005, **73**, 4161.
47 P. Mowlds and K. Kavanagh, *Mycopathologia*, 2007, **165**, 5.
48 P. Mowlds, A. Barron and K. Kavanagh, *Microbes Infect.*, 2008, **10**, 628.
49 E. Mylonakis, R. Moreno, J. B. El Khoury, A. Idnurm, J. Heitman, S. B. Calderwood, F. M. Ausubel and A. Diener, *Infect. Immun.*, 2005, **73**, 3842.
50 R. Rowan, C. Moran, M. McCann and K. Kavanagh, *BioMetals*, 2008, **22**, 461.
51 M. F. Effendy, C. Pettinari, R. Pettinari, A. Pizzablocca, B. W. Skelton and A. H. White, *Inorg. Chim. Acta*, 2006, **359**, 1504.
52 G. W. Eastland, M. A. Mazid, D. R. Russell and M. C. R. Symons, *J. Chem. Soc., Dalton Trans.*, 1980, 1682.
53 Spectroscopic Tools; http://www.science-and-fun.de/tools/
54 Y. Kachkurova, *Theor. Exp. Chem.*, 1967, **3**, 498.
55 G. B. Deacon and R. J. Phillips, *Coord. Chem. Rev.*, 1980, **33**, 227.
56 P. Pyykkö, *Chem. Rev.*, 1997, **97**, 597.
57 C.-S. Liu, P.-Q. Chen, Z. Chang, J.-J. Wang, L.-F. Yan, H.-W. Sun, X.-H. Bu, Z. Lin, Z.-M. Li and S. R. Batten, *Inorg. Chem. Commun.*, 2008, **11**, 159.
58 L. J. Ashfield, A. R. Cowley, J. R. Dilworth and P. S. Donnelly, *Inorg. Chem.*, 2004, **43**, 4121.
59 A. Castiñeiras, I. García-Santos, S. Dehnen and P. Sevillano, *Polyhedron*, 2006, **25**, 3653.
60 R. Rowan, T. Tallon, A. M. Sheahan, R. Curran, M. McCann, K. Kavanagh, M. Devereux and V. McKee, *Polyhedron*, 2006, **25**, 1771.